Part III
Nebular Astrophysics

Contents

1 Atomic processes

1.1 Photoionization

Photoionization

In time-dependent perturbation theory, the rate of transition between two states, $i \rightarrow f$, is:

$$\frac{dP_{if}}{dt} = \frac{e^2}{hc^3 m_e^2} \sum_{\alpha=1}^{2} \int \omega_{fi}\, \mathcal{N}_\alpha(\vec{k})\, |\langle \phi_f | e^{i\vec{k}\cdot\vec{x}} \vec{e}_\alpha \cdot \vec{p} | \phi_i \rangle|^2 \, d\Omega,$$

where $\mathcal{N}(\vec{k})$ is the occupation number of photons in the state corresponding to $\vec{k}$, with frequency ν_{fi}.

In a photoionization process the final states f belong to the continuum. The Born approximation neglects the influence of the ion on $|\phi_f\rangle$, and for a description of the continuum we adopt a hard box normalization, with a size $L \to \infty$. With i corresponding to the fundamental state of the hydrogen atom, we obtain (Shu I, 23),

$$\frac{dP_{if}}{dt} \propto \omega_{fi}^{-3} \mathcal{N}(\omega), \text{ where } \mathcal{N}(\omega) = \int d\Omega \mathcal{N}(\vec{\omega}).$$

.3

Photoionization

The rate of absorption of ionizing photons with frequencies in the range $[\nu, \nu + \nu]$ is $dN_f \frac{dP_{if}}{dt}$, where dN_f is the number of free states in the corresponding range of energies,

$$dN_f = \frac{V}{2\pi^3} 4\pi\, k_e^2\, dk_e,$$

where $\vec{k_e}$ refers to the free electron.

The cross-section of ionization is defined through

$$P_{if} dN_f = t\, \sigma_{if}(\omega) c\, \frac{\mathcal{N}(\vec{n})}{V}\, 4\pi n^2 dn, \text{ with } \frac{d^3\vec{n}}{V} = \frac{d^3\omega}{(2\pi)^3 c^3}.$$

Identifying for $\sigma(\nu)$ we get

$$\sigma(\nu) \propto \nu^{-3} g(\nu),$$

where $g(\nu)$ is a gaunt factor, $g(\nu) \propto \nu^{-1/2}$, in the Born approximation, which is valid far from the ionization edge $\nu_\circ$. $g_\nu \approx 1$ in the vicinity of $\nu_\circ$, where the free-particle approximation breaks down.

.4

The Balmer Jump: photionization of hydrogen

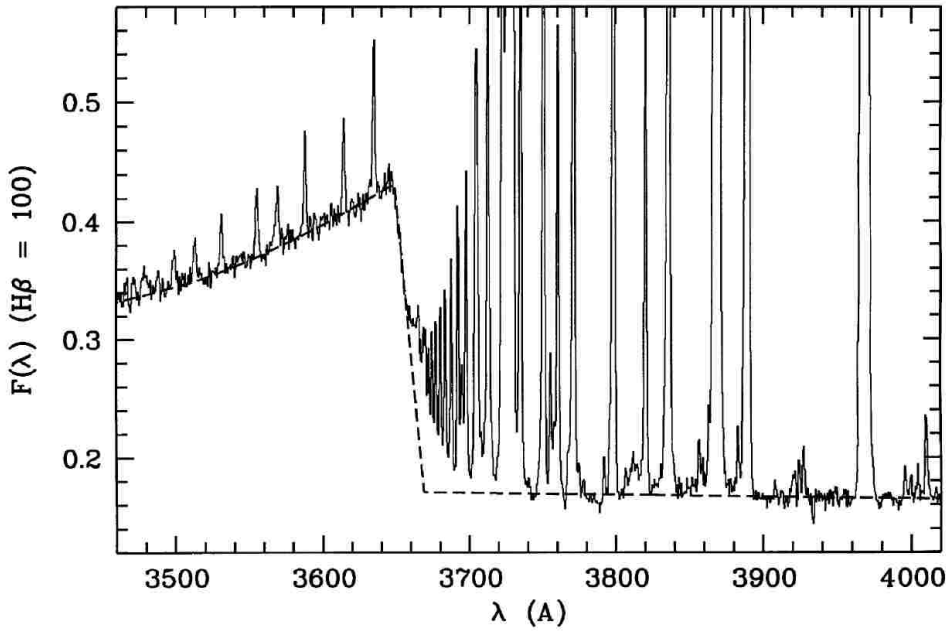

.5

Photoionization of metals[1]

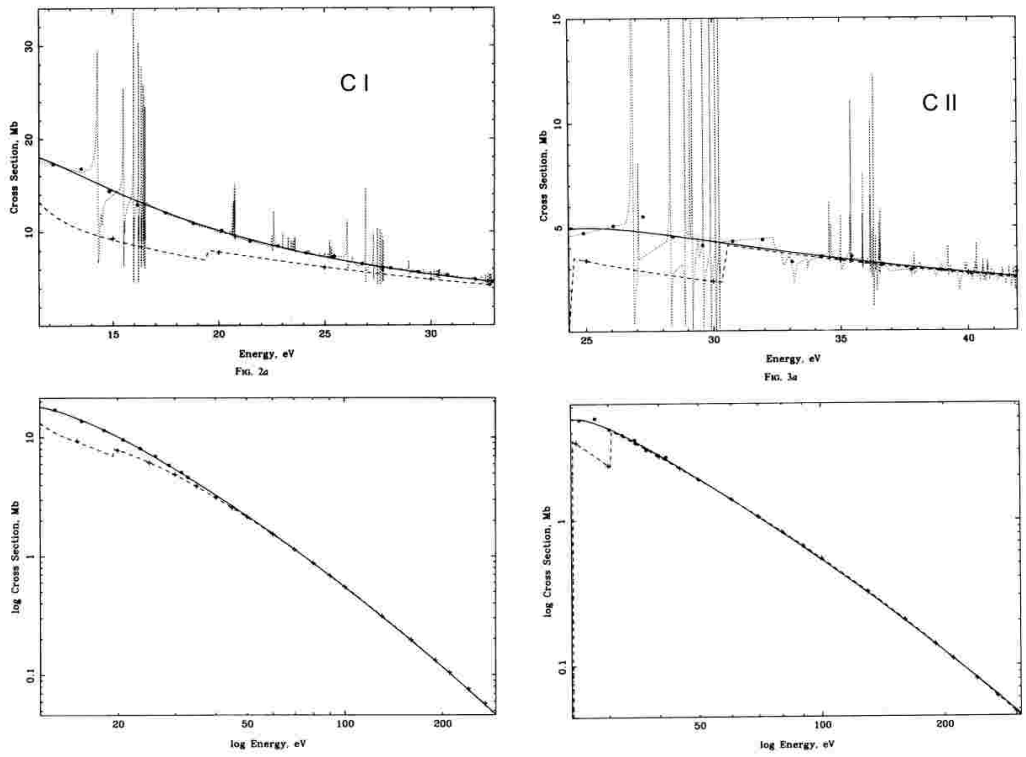

.6

Photoionization of metals: hard X-rays[2]

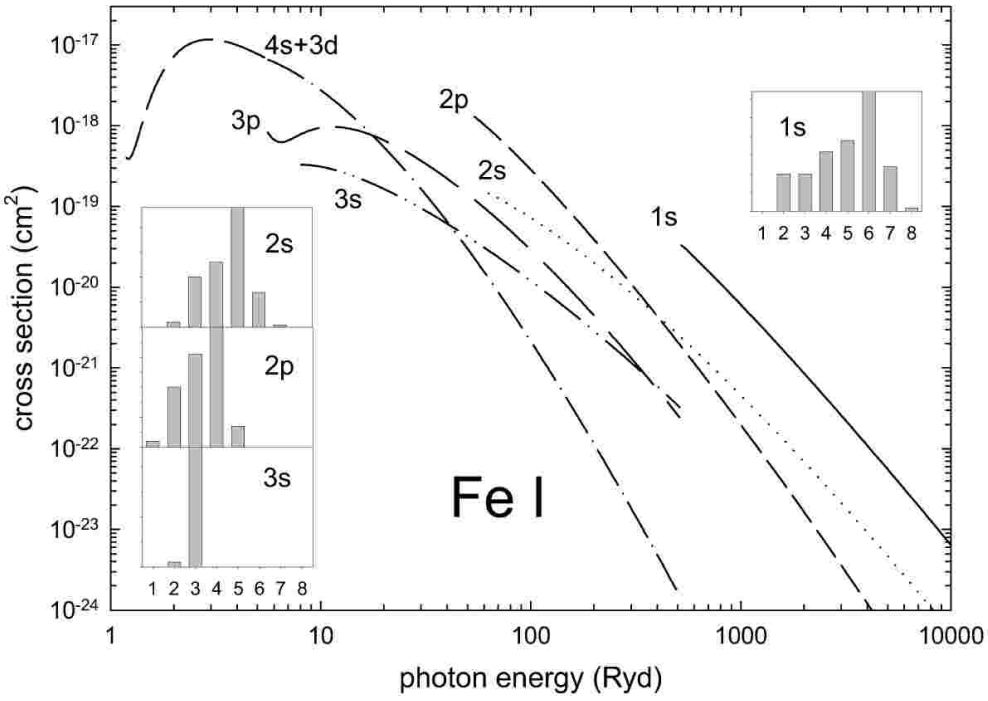

.7

[1] Verner et al. 1996, ApJ, 465, 487. 1 $b = 10^{-24}$ cm^2.

[2] CLOUDY manual, Hazy.

1.2 Collisional Ionization

Collisional Ionization[3]

Direct collisional ionization: $A + e \rightarrow A^+ + 2\,e$

Excitation – auto-ionization: $A + e \rightarrow A^\star + e$

$A^\star \rightarrow A^+ + e$

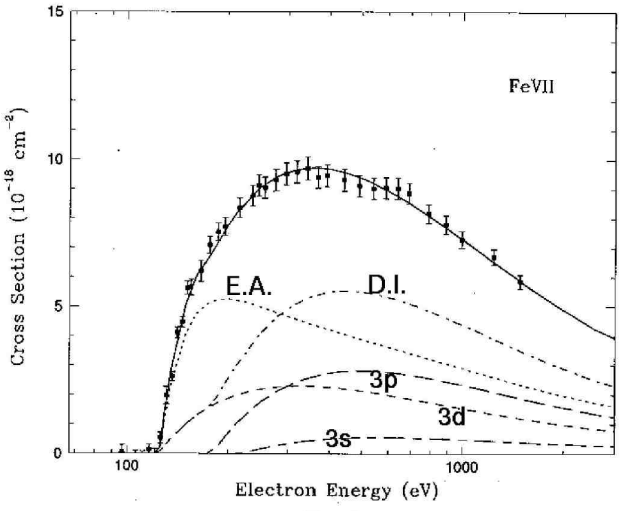

[4]

.8

1.3 Recombination

Radiative recombination

Photoionization and its inverse process, radiative recombination, are related by the Einstein - Milne relations (e.g. Osterbrock, A1; Shu I,75; Spitzer p104)). The detailed balance between photon absorptions with frequency ν and electron-ion recombinations with relative velocity v is

$$n_X\, a_\nu 4\pi \frac{B_\nu}{h\nu}\, d\nu = n_{X^+} n_e v \sigma(v) f(v) dv \;+\; n_{X^+} n_e \sigma_2(v) B_\nu v f(v) dv,$$

where $\frac{1}{2}mv^2 + h\nu_T = h\nu$, and where $f(v)$ is the Maxwellian integrated over angles. We get (tarea) that $\sigma_2 = \sigma/(2h\nu^3/c^2)$, and

$$\sigma(v) = \frac{g}{g_+} \frac{h^2\nu^2}{m^2c^2v^2} a_\nu,$$

where g and g_+ are the degeneracies of X and X^+ in their fundamental levels.

.9

[3] Arnaud & Rothenflug 1985, A&AS, 60, 425; Arnaud & Raymond, ApJ, 1992, 398, 394

[4] the subshell contributions to D.I. are indicated

• Collisional recombination

Recombination through 3 body collisions

$$\mathrm{A}^{+} + 2\,\mathrm{e} \rightarrow \mathrm{A} + \mathrm{e},$$

is important in the limit of very high densities. Note high densities is not the domain of validity of the collisional ionization equilibria, since these assume optically thin conditions. Rather, high densities are simply described by the law of mass-action, as in stellar interiors.

But another domain of validity of 3-body collisions, applicable to the diffuse ISM, is the case of radio recombination lines of H I (e.g. H 109α at 6 cm, see Osterbrock p97). .10

Dielectronic recombination

The inverse process to excitation-autoionization is the dielectronic recombination. For example (e.g. Osterbrock 1989) consider the recombination of C^{++} in its fundamental configuration $1s^2 2s^2\ {}^1\mathrm{S}$ through the collision with a 0.41 eV electron, which matches the energy of C^{+} in $1s^2 2p3d\ {}^2\mathrm{F}$. Doubly excited C^{+} decays following a cascade (in practice 2 photons, through $2s2p^2\ {}^2\mathrm{D}$) to the ground state $1s^2 2s^2 2p\ {}^1\mathrm{P}_{1/2}$. Generically,

$$\mathrm{X}^{+i+1} + e \rightarrow\ {}^{\star}\mathrm{X}^{+i} \rightarrow \mathrm{X}^{+i} + h\nu$$

where ${}^{\star}X^{+i}$ is an autoionizing state of X^{+i}. This is the dominant mechanism for recombination at nebular temperatures of 10^4 K and densities (Nussbaumer & Storey, 1983, A&A, 126, 75). No calculations are available for elements heavier than Ne. .11

1.4 Charge Transfer

Charge transfer

(Spitzer + Osterbrock)

$$A + H^{+} \underset{k_2}{\overset{k_1}{\rightleftharpoons}} A^{+} + H$$

• relationship between the rates of forward and reverse reactions, k_1 and k_2 .12

2 Ionization equilibrium

2.1 Collisional ionization in the low density limit.

Ionization equilibrium - Collisional Ionization

In the limit of low densities, and in the absence of external radiation fields, the relative ionic concentrations are obtained from detailed balance (the example is from Jordan (1969), but the calculations from Arnaud et al. are more recent):

$$\frac{N(X^{+(m+1)})}{N(X^{+m})} = \frac{Q(X^{+m})}{\alpha_{\mathrm{tot}}(X^{+m})},$$

where Q and α_{tot} are the rate coefficients for ionization and recombinations.

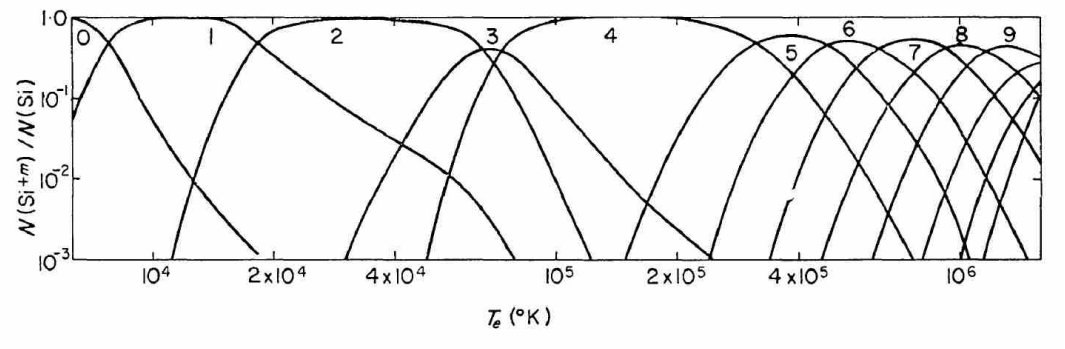

.13

2.2 Photo-ionization equilibrium

Ionization equilibrium - Photoionization

The structure of a photoionized nebula in spherical symmetry can be described by the ionization fraction of each element as a function of nebular radius. For a blob of nebular material, the ionization balance requires that the number of recombinations of ion X^{+i+1} be equal to the number of photoionizations of ion X^{+i},

$$N(X^{i+1})N_e\alpha_T = \int d\nu \frac{4\pi J_\nu}{h\nu} a_\nu N(X^i), \tag{1}$$

where N_e is the electron density, α_T is the total recombination coefficient, and a_ν is the cross-section of photoionization, and J_ν is the local angular average of the nebular specific intensity field,

$$\begin{aligned} J_\nu &= \frac{1}{4\,\pi}\int_{4\pi} I_\nu d\Omega, \\ &= \frac{1}{2}\int_{-1}^{+1} d\mu\; I_\nu(r,\mu), \text{ for spherical symmetry, with} \\ \mu &= \cos\theta, \end{aligned}$$

where the angle θ is measured relative to the radial direction.

.14

3 Thermal Balance

Thermal Balance

(R.E. Williams, en Lecture Notes on Introductory Theoretical Physics).

The electron bath is the specie that thermalizes fastest in an ionized nebula (Spitzer, Cap. II). We consider the energy balance of the electrons.

- **Heating of the electrons**.
- collisional de-excitation. Important in dense nebulae, and partially compensated by collisional excitations.
- photoionization.

.15

Thermal Balance - Photoionization

Each photoelectron yields $\frac{1}{2}mv^2 = h\nu - I$ to the electron bath,

$$G = N_{\rm H}\int_{\nu_1}^{\infty} 4\pi J_\nu a_1(\nu) h(\nu-\nu_1)d\nu = N_{\rm H}\int_{\nu_1}^{\infty} 4\pi J_\nu a_1(\nu) h(\langle\nu\rangle-\nu_1)d\nu,$$

with

$$h\langle\nu\rangle = \int_{\nu_1}^{\infty}\frac{J_\nu}{h\nu}a_1(\nu)h\nu d\nu \Big/ \int_{\nu_1}^{\infty}\frac{J_\nu}{h\nu}a_1(\nu)d\nu.$$

To a good approximation, $a_\nu = a_\circ(\nu_1/\nu)^3$, and in the UV we can use the Wien limit for blackbody radiation:

$$J_\nu \propto \nu^3 \exp\left(-\frac{h\nu}{kT_\star}\right).$$

$$\Rightarrow h\langle nu\rangle = \int_{\nu_1}^{\infty} e^{-\frac{h\nu}{kT_\star}}d\nu \Big/ \int_{\nu_1}^{\infty}\frac{1}{\nu}e^{-\frac{h\nu}{kT_\star}}d\nu \approx h\nu_1 + kT_\star.$$

.16

Thermal Balance - OTS

In a steady state, the equation for photoionization, $\mathrm{H} + \nu \underset{k_2}{\overset{k_1}{\rightleftharpoons}} \mathrm{H}^+ + \mathrm{e}^-$, implies that $k_1 = k_2$. In general the mean specific intensity field $J_\nu(\vec{r})$ contains stellar photons, atenuated radially by nebular absorption, and photons emitted by the nebula. The bulk of the diffuse component is composed of Lyman continuum photons, which can be absorbed by neutral hydrogen in the nebula. In the **On-The-Spot** approximation, the ionization equilibrium $k_1 = k_2$,

$$N(\mathrm{H\,I})\int_{\nu_1}^{\infty} d\nu 4\pi J_\nu a_1(\nu)/h\nu = N_e N(\mathrm{H\,II})\alpha,$$

where α is the total recombination coefficient, can be written

$$N(\mathrm{H\,I})\int_{\nu_1}^{\infty} d\nu 4\pi J^\star_\nu a_1(\nu)/h\nu = N_e N(\mathrm{H\,II})\alpha^{(2)},$$

where $\alpha^{(2)} = \alpha - \alpha_1$.

.17

Thermal Balance - net heating

The cross-section for radiative recombinations is characteristic of Coulomb interactions, $\propto 1/v^2$,

$$\sigma_{\rm rec} = \sigma_\circ(v_\circ/v)^2,$$

which follows from Milne's relation $\sigma_{\rm rec}(v) \approx \nu^2 a_\nu/v^2$, where $h\nu = \frac{1}{2}mv^2 + h\nu_T \approx h\nu_T$, for $T_e < 10^5$ K. Averaging over velocities,

$$\alpha^{(2)} = \langle v\sigma_{\rm rec}\rangle \propto \langle\frac{1}{v}\rangle \propto 1/\sqrt{T_e}.$$

Since the average kinetic energy per photoelectron is $kT_\star$, The net heating is

$$G = N_e N(\mathrm{H\,II})\alpha^{(2)} kT_\star.$$

.18

Thermal Balance - cooling

- **Cooling of the electrons**.

- Collisional excitations.
- Recombinations.

Pure hydrogen nebula

The excited levels of H are at energies that cannot be reached at temperatures typical of photoionized nebulae, 13.6 (1-1/4) eV corresponds to $T \approx 10^5$ K. $\Rightarrow$ cooling by recombinations dominates, i.e.

$$L_R = N_e N(\mathrm{H\,II}) \alpha^{(2)} \frac{1}{2} m \langle v^2 \rangle \propto \sqrt{T_e}.$$

$\Rightarrow$ For a pure hydrogen nebula, $T_e = \frac{2}{3} k T_\star$. .19

Thermal Balance - cooling by metals

Nebulae with metals

The collisional excitation of the fine structure levels (but also with ΔL) of heavy ions, such as S, N, O, C, are close to the ground state, at only $\chi \lesssim 3$ eV. Collisional excitation followed by radiative de-excitation is the main cooling mechanism for ionized nebulae:

$$L_C = N_e N(X^i) \langle \sigma_e v \rangle \chi,$$

with

$$\langle \sigma_e v \rangle = \frac{1}{\sqrt{T_e}} \exp(-\frac{\chi}{k T_e}).$$

.20

4 Nebular models

Nebular models

The abundance ratios of consecutive stages of ionisation, $Q_{X^i} = N(\mathrm{X}^{i+1})/N(\mathrm{X}^i)$, is given by the ionisation equilibrium:

$$N(\mathrm{X}^{i+1}) N_e \alpha_T = \int d\nu \frac{4\pi J_\nu}{h\nu} a_\nu N(\mathrm{X}^i), \qquad (2)$$

provided the ionising field is known.

Given the density field, the structure of a photoionised nebula is computed numerically by progressing outwards in radius. This is the basic principle of the photionisation code CLOUDY, by Gary Ferland et al.. Comparing model and observations of ionic line fluxes is a tool for the study of nebular physical conditions. But the atomic databases are often only approximate, and the uncertainties in the dielectronic recombination propagate from the first stages of ionisation. .21

High-excitation lines in PN NGC 6302

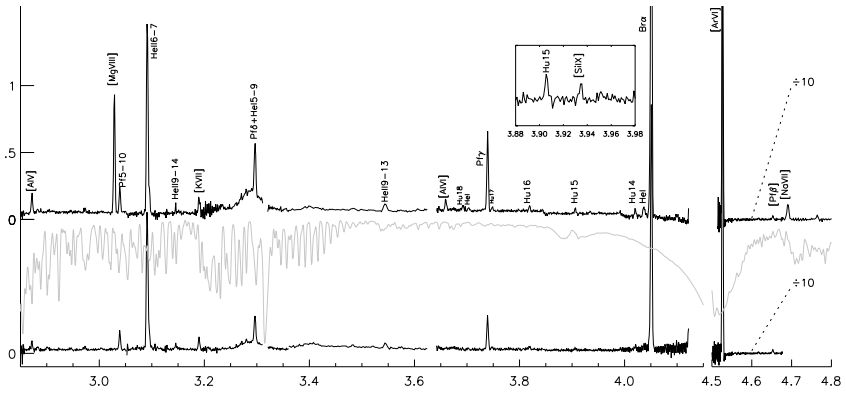

.22

Ionization curves in NGC 6302

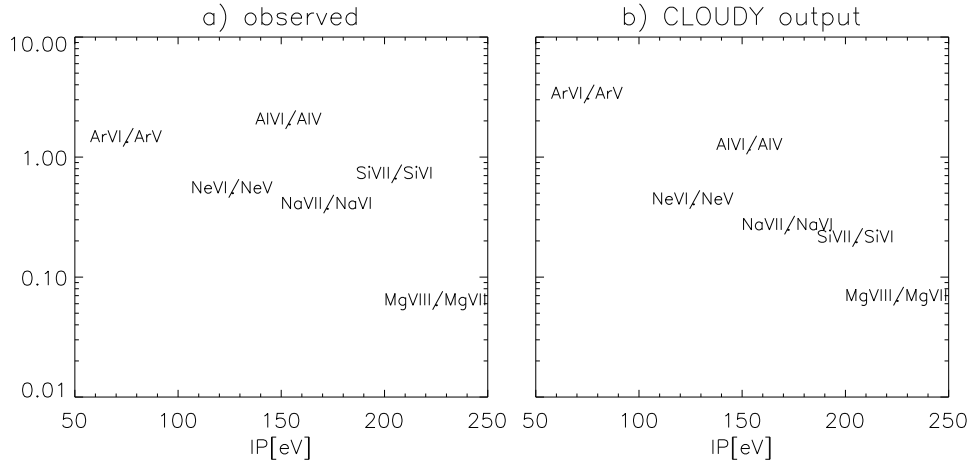

.23

Ionization structure in NGC 6302

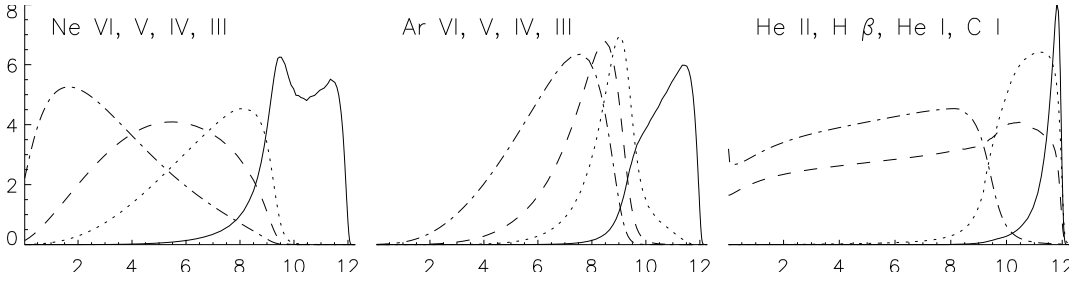

.24

Example input for CLOUDY: `parispn.in`

```
black body, T=150,000K radius = 10 hden = 3.4771213 radius
= 17 normalize to Ca b   4861 abund he -1 C-3.523 N-4.  O-3.222
ne-3.824 mg-4.523
```

Tarea: Run the validation model for CLOUDY 96 called `parispn.in`, and plot the relative abundances of each ionisation stage for H, He and Ne. .25

- Strömgren Spheres
- Pure hydrogen nebulae

(ver Problema 3-1 de Shu I)

- Dusty H II regions.

(Petrosian, Silk & Field, 1972, ApJ, 177, 69; Spitzer)

- Limits of the OTS approximation.

see `dhii.pdf`. .26

3 D

Monte Carlo methods allow calculating the 3D photoionisation structure given a proton density field. The best 3D code available is Mocassin (Ercolano et al. 2003, MNRAS, 340, 1136).

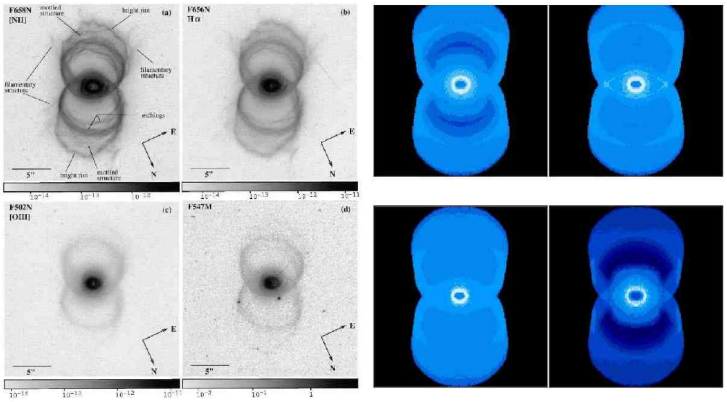

Figure 1: *Left Panel*: From Sahai et al. 1999. Narrow-band HST WFPC2 images of MyCn 18: (a) F658N ([N II]λ6586; (b) F656N (Hα); (c) F502N ([O III]λ5007); (d) a continuum fi lter F547N. *Right panel*: From Ercolano et al. (in prep.). 2D projections of 3D emissivity grids obtained from our best-fi tting MOCASSIN model of MyCn18: (a) [N II]λ6586; (b) Hβ); (c) [O III]λ5007; (d) [O I]λ6300.

.27

5 Temperature and density diagnostics

5.1 Recombination lines

Temperature and density diagnostics

- **Recombination lines of H I, He II, and He I**

The flux of a hydrogen recombination line in the optical is $F_{ij} = \int ds d\Omega j_{ij}$, where the emissivity of a transition $n_i \leftarrow n_j$ populated by the recombination cascade is

$$j_{ij} = \frac{h\nu}{4\pi} \sum_{L_i=0}^{n-1} \sum_{L_j=L_i\pm1} N_n h\nu_{ij}.$$

The occupation numbers N_n can be calculated, and bear a weak dependence on T_e, N_e. The radiative transfer effects are included through an OTS approximation that distinguishes two cases (Baker & Menzel 1938, ApJ, 88, 52): case A, where the nebula is optically thin in every transition (as well as in the Lyman continuum), and case B where all photons from the Lyman serie, as well as the Lyman continuum, are absorbed OTS, so that the effective fundamental state in the recombination cascade is $n = 2$. .28

Optical Recombination Lines - ORLs

The effective recombination coefficient is defined through

$$N_p N_e \alpha_{ij}^{\rm eff} = \frac{4\pi}{h\nu_{ij}} j_{ij}.$$

Hummer & Storey (1987, MNRAS, 224, 801) give $\alpha_{\rm H\beta}^{\rm eff} = 3.0\ 10^{-14}$ cm^{-3}, at 10^4 K (approximately $\propto \sqrt{1/T_e}$), and tabulate the emissivities of H I and He II recombination lines relative to H_β. The relative emissivities for the He I recombination lines are tabulated by Smits, MNRAS, 251, 316. Those of O II, N II, N III, Ne II, C II y C III have been computed by Storey et al. and can be found in the recent literature.

Note that given N_e and the flux of a recombination line, it is straightforward to obtain the column of the corresponding ion. For example the recombination spectrum of O II gives the column of O^{2+}, which has the spectrum of O III. .29

5.2 Collisionally Excited Lines - CELs.

Collisionally Excited Lines - CELs.

The flux of an optically thin CEL $i \leftarrow j$ is given by integrating the line emissivity along the optical path s:

$$F_{ij} = \int ds \int d\nu\, d\Omega\ j_\nu = \int ds\, d\Omega\ \frac{A_{ij} h\nu_{ij}}{4\pi} N_j,$$

where N_j is the population of the excited level j.

The principle underlying the diagnostic of physical conditions in ionised nebulae is the dependence of $N_j(\vec{r})$ on T_e, N_e. Neglecting radiative excitations (i.e. optically thin case),

$$\sum_{i\neq j} n_j C_{ji} + \sum_{i<j} n_j A_{ji} = \sum_{i\neq j} n_i C_{ij} + \sum_{i>j} n_i A_{ij},$$

where $N_j = n_j N_\circ$, and $N_\circ$ is the ground state population. In LS coupling the Hund rules give 2 to 5 levels in the fundamental configuration of common ions. .30

5.3 Temperature and density.

Density-sensitive pairs of lines

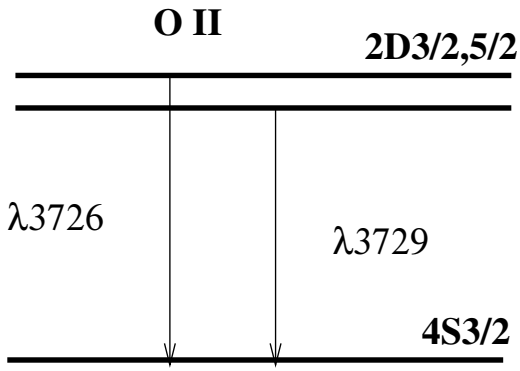

The critical densities of both lines are $N_c(\lambda 3729) = 4\,10^{13}\mathrm{cm}^3$ and $N_c(\lambda 3726) = 2\,10^4\mathrm{cm}^{-3}$, both comparable to typical nebular densities. The ratio of these lines does not depend on the concentration of O^+. Since the upper levels are very close in energy, their relative populations are insensitive on temperature. The [O II] doublet is a good diagnostic for densities close to the critical densities.

.31

density

[O II] doublet for typical densities:

- $N_e \ll N_c$.

$$\frac{I(\lambda 3279)}{I(\lambda 3726)} = \frac{N_e N_1 \langle \sigma_{12} v \rangle \frac{h\nu_{21}}{4\pi}}{N_e N_1 \langle \sigma_{13} v \rangle \frac{h\nu_{31}}{4\pi}} = \frac{\langle \sigma_{12} v \rangle}{\langle \sigma_{13} v \rangle},$$

  independent of N_e[5]
- $N_e \gg N_c$. In this case $N_3 = N_1 C_{13}/C_{31} = N_1 g_3 e^{-\chi_3/kT}/g_1$ and

$$\frac{I(\lambda 3279)}{I(\lambda 3726)} = \frac{A_{21} N_2 g_2}{A_{31} N_3 g_3},$$

  independent of N_e and weakly dependent on T_e.
- In an intermediate case, we consider $N_c(\lambda 3729) \ll N_c \ll N_c(\lambda 3726)$:

$$\frac{I(\lambda 3279)}{I(\lambda 3726)} = \frac{g_2}{g_3} \frac{A_{21}}{N_e \langle \sigma_{12} v \rangle} \propto \sqrt{T_e}/N_e,$$

  which is a function of N_e.

.32

Temperature-sensitive pairs

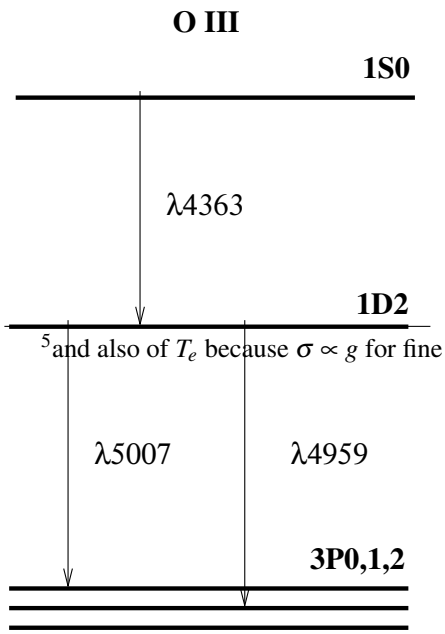

These 3 transitions have $A \gtrsim 1\ \mathrm{s}^{-1}$, $N_c \gg 10^4\ \mathrm{cm}^{-3}$, and $A_{32} \ll A_{31}$, so that

$$\begin{aligned} j(\lambda 4363) &= N_e N_1 \langle \sigma_{13} v \rangle \frac{h\nu_{32}}{4\pi}, \\ j(\lambda 5007) &= N_e N_1 \left[\langle \sigma_{12} v \rangle + \right. \\ &\quad \left. \langle \sigma_{13} v \rangle \frac{A_{32}}{A_{31} + A_{21}} \right] \frac{h\nu_{21}}{4\pi}, \end{aligned}$$

[5] and also of T_e because $\sigma \propto g$ for fine structure levels

where we have treated $\lambda 4959$ and $\lambda 5007$ as a single line. The ratio of these **two** lines is

$$\frac{I(\lambda 5007)}{I(\lambda 4363)} = \frac{\lambda_{32}}{\lambda_{21}}\left[1+\frac{\langle\sigma_{12}v\rangle}{\langle\sigma_{13}v\rangle}\right].$$

Remembering that $\langle\sigma_{ij}v\rangle \propto T_e^{-1/2}e^{-\chi_{ij}/kT_e}$, we see that the ratio $\frac{I(\lambda 5007)}{I(\lambda 4363)}$ is sensitive on the temperature. One gets $I(\lambda 5007)/I(\lambda 4363) \approx 8\ \exp(33000/T_e)$. .33

Density and the ORLs

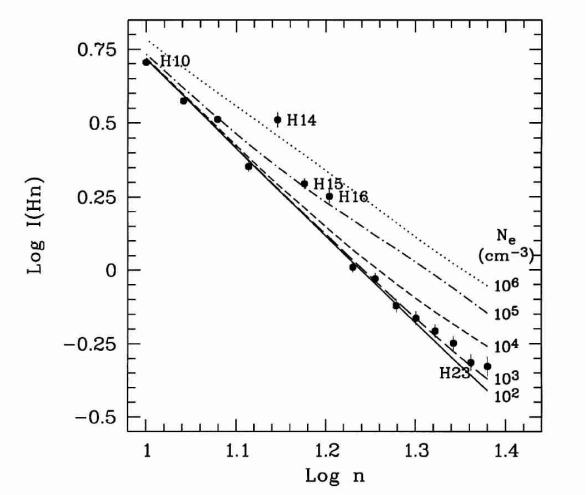

The recombination lines have a very weak dependence on density, which can be used as diagnostic (Liu et al. 2000, MNRAS, 312, 585). .34

5.4 The line-continuum-temperature relationship

The line-continuum-temperature relationship

The radio-continuum flux density of free-free radiation relates to the Hβ flux through

$$F(H\beta) = 0.28T_e^{-0.52}\nu^{0.1}F_\nu,$$

which gives T_e. The recombination lines with $n \gg 1$ at radio frequency are not extinct, and their emissivities can be calculated in LTE (the correction is $\ll 1$ and is tabulated by Brocklehurst 1970, MNRAS 148, 417). .35

Balmer and Paschen discontinuity

$BJ = \frac{I_c(\lambda 3643) - I_c(\lambda 3681)}{I(H11,\lambda 3770)}$.
$I_c(\lambda)$ is tabulated by Brown & Mathews (1970, ApJ, 160, 939).

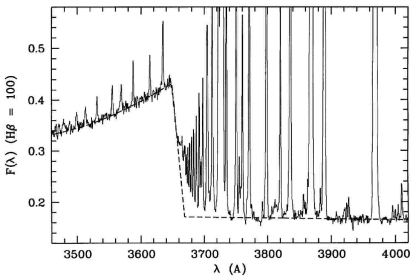

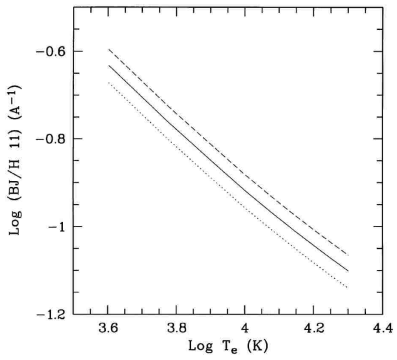

He^+/H^+ = 0.1, He^{++}/H^+=0 (dots);
He^+/H^+ = He^{++}/H^+=0.05 (solid);
He^+/H^+ = 0, He^{++}/H^+=0.1 (dashed).

The same analysis can be applied to the Paschen discontinuity at 8194Å. .36

5.5 The ORL/CEL discrepancy

The ORL/CEL discrepancy

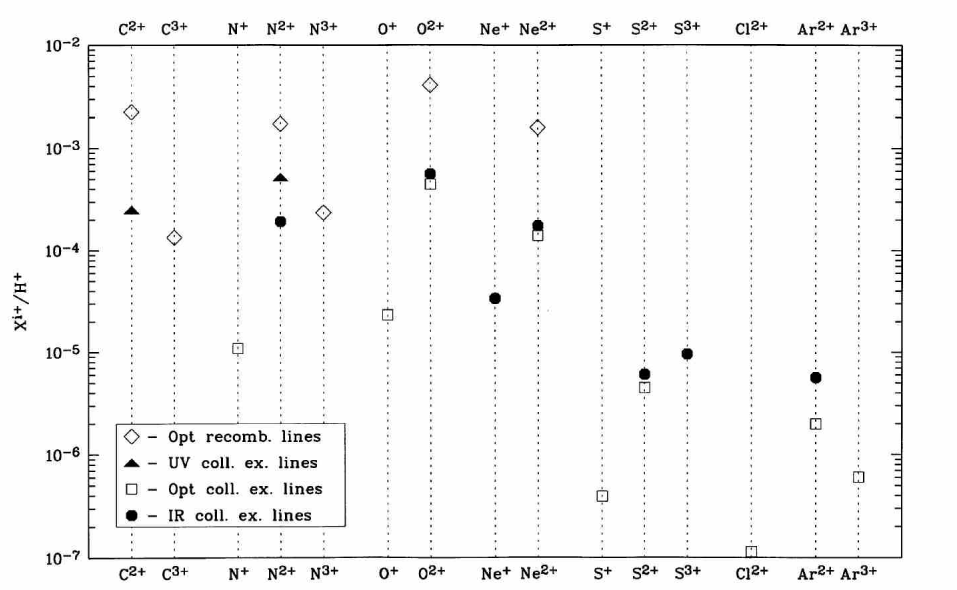

.37

ORL/CEL

- In principle the best indicators of ionic abundances are the ORLs, because the recombination coefficients of both hydrogen and metals are approx. $\propto 1/\sqrt{T_e}$, so that the residual dependence on temperature is very weak.
- The difficulty with ORLs is that their fluxes are $10^{-3} - 10^{-4}$ weaker than Hβ.
- By contrast the CELs have an exponential dependence on temperature, and their fluxes are comparable to Hβ.

.38

ORL/CEL

Table 8: Comparison of ORL and CEL temperatures [K] and abundances

Nebula	T_e([O III]) CEL	T_e(BaJump) ORL	T_e(He I) ORL	T_e(O II) ORL	Abundance ORL/CEL
NGC 7009	9980	8150	5380	1800	4.7
M 2-36	8380	5900	4160	1180	6.9
NGC 6153	9120	6080	3370	1180	9.2
M 1-42	9220	3560	2310	$\leqslant$200	22
Hf 2-2	8820	900	775	360	84

There is a systematic discrepancy between CELs and ORLs:

- $T_e(\text{CEL}) > T_e(\text{ORL} \sim T_e(\text{continuum})$
- $N(X^{+i})(\text{CEL}) < N(X^{+i})(\text{ORL})$, although the columns are similar when using the same temperatures.

.39

ORL/CEL discrepancy - temperature fluctuations.

One strategy to reconcile the temperature discrepancy, original proposed by Peimbert (1967, ApJ, 150, 825) to explain the systematic discrepancy in $T(\text{O III})$ and $T(\text{continuum})$, is the "t^2" formalism. In this formalism one expands the CEL emissitivies in small temperature fluctuations about a mean value:

$$j(T) = j(T_\circ) + (T - T_\circ)\left.\frac{dj}{dT}\right|_{T=T_\circ} + \frac{1}{2}(T - T_\circ)^2 \left.\frac{d^2 j}{dT^2}\right|_{T=T_\circ}, \text{and,}$$

$$\int N_e N_i j(T) ds = j(T_\circ) \int N_i N_e ds + \frac{1}{2}\left.\frac{d^2 j}{dT^2}\right|_{T=T_\circ} \int ds N_i N_e (T - T_\circ)^2,$$

where the term of order 1 cancels out when choosing

$$T_\circ = \int ds N_i N_e T \Big/ \int ds N_i N_e. \quad \text{We define } t^2 = \frac{\int N_i N_e (T - T_\circ)^2 ds}{T_\circ^2 \int ds N_i N e}.$$

Two pairs of T_e-sensitive lines allow calculating $T_\circ$ and t^2. In this formalism $T_\circ$ is **the** nebular temperature, and is closer to the ORLs and to the continuum than to the CELs. In other words t^2 effectively adopts the ORL values.

.40

ORL/CEL discrepancy - solution?

An alternative to the t^2 formalism is to interpret the observed discrepancies as real, and conclude there are cold and metal rich inclusions in the nebulae. These inclusions may find their origin in the evaporation of globules or ices on big-grains (or planetesimals) for H II regions, or in the ejection of enriched stellar material in the dredge-up of AGB precursors to planetary nebulae.

Table 8: Comparison of ORL and CEL temperatures [K] and abundances

Nebula	T_e([O III]) CEL	T_e(BaJump) ORL	T_e(He I) ORL	T_e(O II) ORL	Abundance ORL/CEL
NGC 7009	9980	8150	5380	1800	4.7
M 2-36	8380	5900	4160	1180	6.9
NGC 6153	9120	6080	3370	1180	9.2
M 1-42	9220	3560	2310	$\leqslant$200	22
Hf 2-2	8820	900	775	360	84

.41

ORL/CEL discrepancy - solution?

Photoionisation models with two phases indicate that the bulk of nebular material should come from the 'hot' component, which is traced by the CELs (good news!). A test for this interpretation is to study the thermal broadening of the ORLs, as observed by Barlow et al. (astro-ph/0605235), who compared [O III] 4363Å with the sum of the O II ORLs at 4089Å, 4275Å and 4349Å:

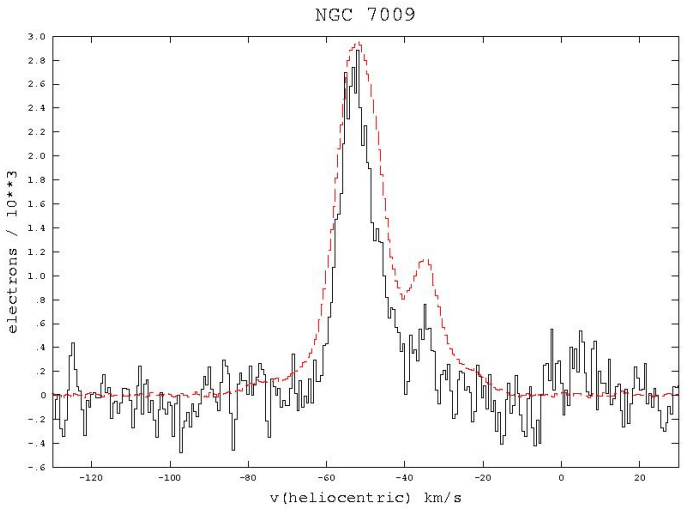

.42